Lab on a Chip

Cite this: *Lab Chip*, 2011, **11**, 3365

www.rsc.org/loc

TECHNICAL NOTE

Parallel sub-micrometre channels with different dimensions for laser scattering detection

Stefano Pagliara,†[a] Catalin Chimerel,†[a] Richard Langford,[a] Dirk G. A. L. Aarts[b] and Ulrich F. Keyser*[a]

Received 10th May 2011, Accepted 11th July 2011
DOI: 10.1039/c1lc20399a

A novel and simple approach for the realization of polymer sub-micrometre channels is introduced by exploiting replica molding of Pt wires deposited by focused ion beam. We fabricate arrays of parallel channels with typical dimensions down to 600 nm and with variable height. We characterize the pressure-driven transport of polymer colloids through the channels in terms of the translocation frequency, amplitude and duration by implementing a laser scattering detection technique. We propose a prototype application of the presented platform such as the *in situ* sizing and sensing of populations of particles with different dimensions down to 50 nm.

Introduction

The increasing worldwide demand of rapid low cost and reliable screening has represented a tremendous push toward the miniaturization of lab-on-a-chip devices. They are envisioned as new instrumentation for clinical analysis,[1] chemical sensing[2] and on-chip particle synthesis.[3] Restrictions for mass production and low cost requirements often allow to have only a fixed thickness on the same chip. The most common fabrication approach is soft lithography[4] on structures fabricated by photolithography. Different approaches are used to fabricate microfluidic channels with variable size on a same chip such as laser micromachining,[5] electron beam and photolithography,[6] multilayer soft lithography,[7] gray-tone lithography,[8] stereolithography,[9] solid-object printing.[10] Recently polydimethylsiloxane (PDMS) based complex microchannels have been realized by using fibers[11,12] or plastic tubings and silica capillaries[13] as embedded templates. However, there are fewer approaches[14,15] allowing for polymer sub-micrometre channels with variable height on one microfluidic chip. Focused ion beam (FIB) microfabrication offers a flexible approach toward the realization of silicon or metal printhead master nanopatterns as a mold for soft-lithography.[16,17] FIB has a number of advantages such as high sensitivity and direct fabrication in selective areas without any etch mask. FIB milling has been previously exploited for the fabrication of nanofluidic channels[18] and microfluidic devices.[15,19,20]

Single particle flow control,[21] counting, sizing[22] and manipulation[23] in microfluidic systems is of paramount importance in a huge number of different fields such as environmental, industrial and clinical analysis,[24] chemical and biological sciences,[25] biophysics and fundamental physics studies.[26] Among other single particle detection approaches - such as Coulter counter with nanocapillaries,[27] electrical impedance,[28] laser-induced fluorescence,[29] particle tracking[30,31] and correlation spectroscopy,[31,32] laser scattering is a simple non-invasive label-free method. Laser scattering can be realized at relatively low cost and in portable equipment and allows for the counting and sizing of particles down to the 100 nm scale.[22,33,34]

Here we present a novel approach to fabricate arrays of PDMS sub-micrometre channels of different height by using Pt wires deposited *via* FIB as molds for soft lithography. We test the feasibility of using the channels for microfluidics by studying the pressure-driven transport of single polymer colloids. Our results are well described by the Hagen-Poiseuille flow. We characterize translocations of single particles (with sizes down to 50 nm) in terms of event duration, amplitude and frequency by exploiting laser scattering in a restricted region of a single channel which involves a volume of liquid of a few fL. We demonstrate the *in situ* sizing and sensing of populations of colloids with different dimensions.

Experimental details

Materials and microfluidic chip fabrication

Si (100) wafers and borosilicate glass cover slips are from Compart Technology Ltd (Peterborough, UK) and Glaswarenfabrik Karl Hetch KG (Sondheim, Germany), respectively. AZ 9260 and Sylgard 184 polydimethylsiloxane (PDMS) from Microchemicals GmbH (Ulm, Germany), and Dow Corning (Midland, MI). Polyether ether ketone (PEEK) tubing and shut off valves are from Kinesis (St Neots, UK). Polystyrene (PS) nanospheres with mean diameter (52 ± 8) nm and (457 ± 11) nm

[a]*University of Cambridge, Cavendish Laboratory, Cambridge, CB3 0HE, United Kingdom. E-mail: ufk20@cam.ac.uk; Fax: +44 (0) 1223 337000; Tel: +44 (0) 1223 337272*
[b]*Department of Chemistry, Physical and Theoretical Chemistry Laboratory, University of Oxford, South Parks Road, Oxford, OX1 3QZ, United Kingdom*
† These authors contributed equally to this work.

dispersed in a 2.67 and 2.63% solids (w/v) aqueous suspension, respectively, are from Polysciences (Warrington, PA). In addition poly(methyl methacrylate) (PMMA) nanospheres with mean diameter (290 ± 55) nm are synthesized by means of emulsion polymerization[35,36] and dispersed in a 2.63% solids (w/v) aqueous suspension. Colloidal suspensions are made in a KCl solution with molarity in the range 5–50 mM. Ultrapure water (Synergy System, Millipore Corp., Billerica, MA) is used in the buffer preparation and the buffer is filtered twice through mixed cellulose esters (Medical Millex-GS Filter, 0.22 μm, Millipore Corp.). Finally a dilution of colloid solution in buffer is realized with a volume/volume ratio in the range of 1 : 100 to 1: 4200.

The FIB assisted deposition of the Pt wires (Fig. 1a) is carried out with a Cross-beam 1540 FIB/SEM system (Zeiss, Oberkochen, Germany) equipped with a Ga^+ beam. A typical Pt deposition is carried out by using an accelerating voltage of 30 kV and a beam current of 100 pA. The scanning frequencies are 20 000 and 200 Hz along the longitudinal and orthogonal wire axis, respectively. Arrays of parallel wires with different cross section are typically deposited in a serial way on a same substrate (Fig. 1b). SEM imaging is carried out with an acceleration voltage in the range of 5–30 kV. Conventional photolithography (Fig. 1c) is carried out on a 12 μm-thick AZ 9260 film deposited on the Pt wires by exploiting a MJB4 mask aligner (Karl Suss, Garching, Germany) and a Cr/quartz mask (Photodata Ltd, Hitchin, UK). Replica molding of the resulting device (Fig. 1d) is realized by casting on it a 9 : 1 (base:curing agent) PDMS mixture and *in situ* curing at 60 °C for 40 min in oven (Fig. 1e). The resulting device (Fig. 1f) is made of two inlet and outlet reservoirs separated by a 15 μm-wide and 12 μm thick PDMS wall and connected through three hollow channels with square cross section of 0.36, 1.44 and 3.24 μm^2. PDMS is bonded to a glass slide by exposing both surfaces to oxygen plasma treatment (8.5 s exposure to 2.5 W plasma power, Plasma etcher, Diener, Royal Oak, MI) thus improving adhesion quality and hydrophilicity.[37] The device is completed by the integration of PEEK tubing and shut off valves on their turn connected to a computerized pressure-based flow control system (MFCS-4C, Fluigent, Paris, France) that allows to regulate the flow in the microfluidic chip.

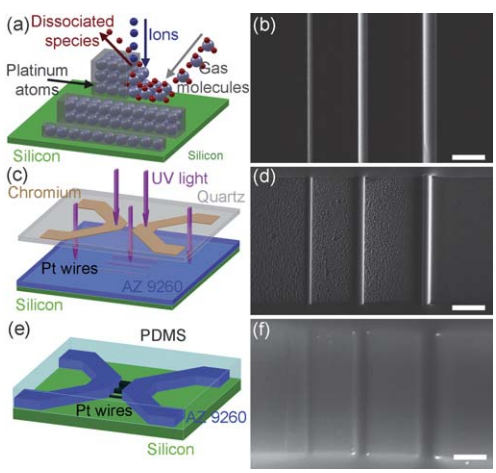

Fig. 1 Fabrication of the microfluidic chip. (a) Focused ion beam deposition of (b) Pt wires with square cross section of 0.36, 1.44 and 3.24 μm^2 from left to right, respectively. (c) Photolithography patterning of an AZ 9260 layer spun-cast on the wires and (d) resulting device with a 15 μm long separation gap. (e) Replica molding by PDMS casting and *in situ* curing and (f) resulting PDMS negative replica. Scale bars: 5 μm.

Laser scattering detection set-up

A diode laser (635 nm, Coherent Inc., Santa Clara, CA) is coupled into an oil immersion objective (100×, 1.4 N.A., UPLSAPO Olympus, Center Valley, PA) and thus focused in a small region of one microchannel (Fig. 2a) with an effective detection volume around 1 fL. The scattered laser-light back-reflected toward the objective is coupled to a four quadrant photodiode. The voltage signal is amplified by a custom-made amplifier and digitized with a NI-PCIe-6251 card (National Instruments (NI), Austin, TX). For recording we use a custom-made program based on LabVIEW (NI) and a sampling rate in the range 100–200 kHz. Pressure-driven translocations of colloids appear as increases in the recorded voltage (peaks in Fig. 2b) and are isolated from the trace by using a custom-made program (LabVIEW 8.6, National Instruments). No

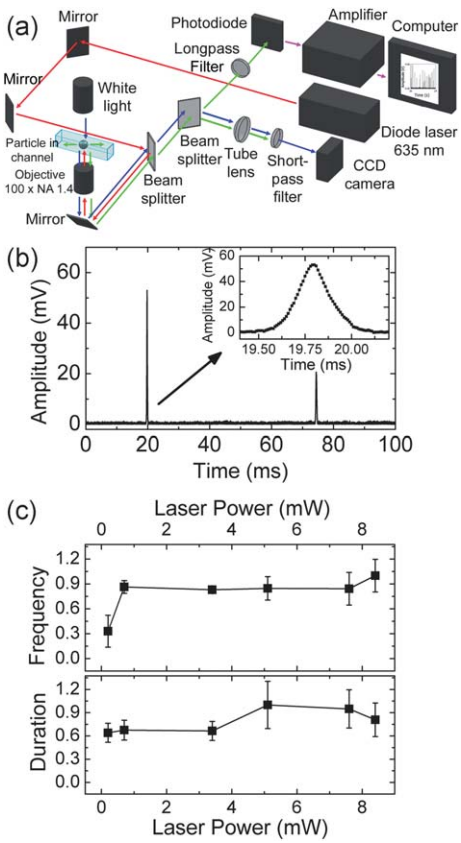

Fig. 2 Light-scattering detection. (a) Detection set-up: the incident and reflected laser beam and the transmitted white light are represented by the red, green and blue arrows, respectively. (b) 100 ms acquisition of the scattering signal from 300 nm colloids flowing in a 1.2 μm-wide channel under a pressure gradient around 40 mbar. Inset: scattering signal from a single colloid. (c) Normalized frequency (top) and duration (bottom) of the colloid translocations, under the same conditions in (b), in dependence of the incident laser power.

translocations are detected when a plain buffer solution is injected in the channel under the same gradient for several minutes in agreement with dynamic light scattering (DLS) measurements carried out by a Zetasizer (Malvern, PA).

Visual inspection is carried out by coupling broadband white light to the microfluidic chip and focusing the transmitted light on a charged-coupled device camera (DMK 21F04, Imaging Source).

Results and discussion

The laser scattering detection is tested on a 300 nm PMMA colloid suspension (5mM KCl) flowing in a channel with square cross section of 1.44 μm^2 under an applied pressure gradient of 40 mbar. Above 0.7 mW the translocation frequency does not vary significantly (top of Fig. 2c). Therefore a sub-mW laser power is sufficient for translocation detection rendering the approach suitable for portable applications. Interestingly the event duration (bottom of Fig. 2c) is not affected by the incident laser power highlighting the absence of any laser-induced trapping effect. The direction of single colloid flow inside the chip is controlled by the external pressure-based system and is tracked on the camera. When a negative pressure gradient is applied colloids flow from the outlet to the inlet reservoir resulting in a negative translocation frequency (Fig. 3a). The flow direction is then reversed by applying a positive pressure gradient and the translocation frequency almost monotonously increases with the applied pressure. The Hagen-Poiseuille model can be applied to our system since the Reynolds number of the flow is sufficiently small (Re < 0.07)[38] and the translocation frequency can be described by:

$$f = cnQ = c\frac{6W}{\rho\pi d^3}\frac{h^3 w\Delta p}{12\eta L}\left[1 - 0.63\frac{h}{w}\right] \quad (1)$$

where Q is the volumetric flow rate, L, h and w are the channel length, height and width, respectively, η the dynamic viscosity of the flowing solution, Δp is the pressure gradient across the channel, n is the number of particles per unit volume, W is the polymer concentration, d is the particle diameter, ρ the polymer density and c is the fraction of volume occupied by the laser spot in the microchannel:

$$c = \frac{V_{Laser}}{V_{Channel}} = \frac{\frac{4}{3}\pi a^3}{w^3} \quad (2)$$

where a is the radius of the laser spot. Calculated values for c are 1.0, 0.89 and 0.28, for 0.6, 1.2 and 1.8 μm wide channel, respectively. Corresponding frequency predictions are reported in Fig. 3a.

The sizing capability is demonstrated by two different experiments carried out on 50 and 300 nm particles under similar conditions. In the scatter plot showing the duration and amplitude of 600 translocations (Fig. 3b) two separated regions are evident; in fact the population of the smallest particles show translocating events with low signal amplitude (2.5 ± 0.5) mV and short duration (0.07 ± 0.02) ms while the largest particles give higher amplitudes (31.0 ± 22.6) mV and longer durations (0.12 ± 0.05) ms. The larger standard deviation for the quantities regarding the PMMA colloids is mainly due to the larger particle size polydispersity with respect to the PS ones as measured by DLS (290 ± 55 nm, black line and 55 ± 5 nm, red line, respectively, in the inset of Fig. 3b). The light scatter distribution can be further broadened by external noise sources.[39]

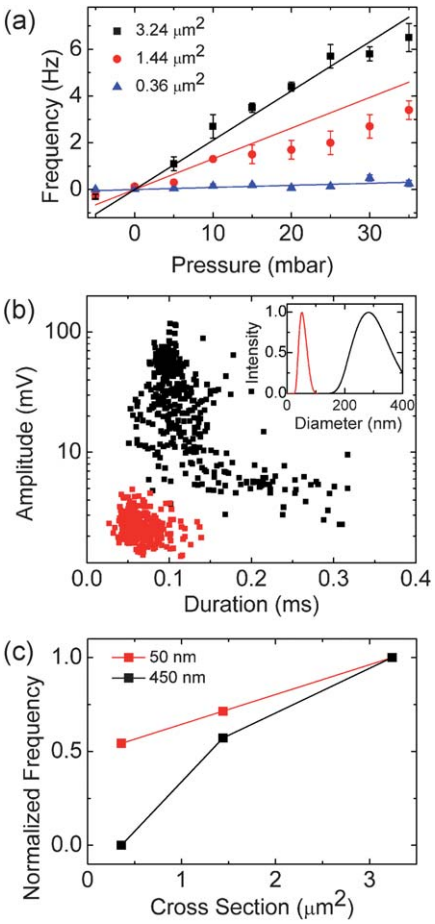

Fig. 3 (a) Translocation frequency with respect to the applied pressure. The error bar is the standard deviation calculated by averaging over measurements acquired for interval of 30 s. The lines are the corresponding predictions by eqn (1). (b) Scatter plot showing the duration and amplitude of 300 translocations of 50 nm (red) and 300 nm (black) colloids. Inset: corresponding DLS measurements on 50 nm (red curve) and 300 nm (black curve) particle suspensions. (c) Normalized translocation frequency for 50 nm (red squares) and 450 nm colloids (black squares) with respect to the channel cross section.

The detection of particles over a critical dimension is easily achieved by exploiting channels with different cross section on the same microfluidic chip. 50 nm particles are initially injected and detected. Thereafter a small amount of 450 nm particles (around 1 : 100 w/w ratio with respect to the 50 nm ones) is injected and the translocations of both types of particles are recorded and reported in a scatter plot similar to the one in Fig. 3b. Each translocation is easily assigned to one of the two particle populations since 50 nm colloids are characterized by a significantly smaller scattering amplitude (<10 mV) with respect to 450 nm ones (>30 mV). The translocation frequency through three different channels is measured for both the populations: while the smallest particles (red squares in Fig. 3c) reach the outlet reservoir by travelling through the three channels

the biggest particles (black squares) go through the medium and the biggest channel but do not travel across the smallest one.

Conclusions

We demonstrated a novel, simple and versatile approach for the realization of polymer-based arrays of sub-micrometre channels with dimension down to 600 nm and with different dimensions on the same microfluidic chip. We have coupled laser scattering in channels for the *in situ* detection of single translocating species with minimum detectable particle size of 50 nm. The presented approach could open the way for the study of transport phenomena of nanoparticles in artificial channels or living systems. The transport could be driven by pressure/concentration gradients or electro-osmotic/phoretic forces and allows for analysis of single particle events.

Acknowledgements

We gratefully acknowledge Eric Tapley and Vito Foderà for their precious help with FIB and DLS. C.C. and U.F.K. were supported by the Emmy Noether program of the Deutsche Forschungsgemeinschaft and an ERC starting grant, respectively. S. P. acknowledges financial support by the Cavendish Laboratory, University of Cambridge.

Notes and references

1 A. Kummrow, J. Theisen, M. Frankowski, A. Tuchscheerer, H. Yildirim, K. Brattke, M. Schmidt and J. Neukammer, *Lab Chip*, 2009, **9**, 972.
2 W. Lee, W. Fon, B. W. Axelrod and M. L. Roukes, *Proc. Natl. Acad. Sci. U. S. A.*, 2009, **106**, 15225.
3 W. Li, J. Greener, D. Voicu and E. Kumacheva, *Lab Chip*, 2009, **9**, 2715.
4 D. C. Duffy, J. C. McDonald, O. J. A. Schueller and G. M. Whitesides, *Anal. Chem.*, 1998, **70**, 4974.
5 D. B. Wolfe, J. B. Ashcom, J. C. Hwang, C. B. Schaffer, E. Mazur and G. M. Whitesides, *Adv. Mater.*, 2003, **15**, 62.
6 S.-Y. Jung, S. T. Retterer and C. P. Collier, *Lab Chip*, 2010, **10**, 2688.
7 H. Wu, T. W. Odom, D. T. Chiu and G. M. Whitesides, *J. Am. Chem. Soc.*, 2003, **125**, 554.
8 J. Chung and W. Hsu, *J. Vac. Sci. Technol., B: Microelectron. Nanometer Struct.–Process., Meas., Phenom.*, 2007, **25**, 1671.
9 Y. Mizukami, D. Rajniak, A. Rajniak and M. Nishimura, *Sens. Actuators, B*, 2002, **81**, 202.
10 J. C. McDonald, M. L. Chabinyc, S. J. Metallo, J. R. Anderson, A. D. Stroock and G. M. Whitesides, *Anal. Chem.*, 2002, **74**, 1537.
11 M. K. S. Verma, A. Majumder and A. Ghatak, *Langmuir*, 2006, **22**, 10291.
12 D. Tu, S. Pagliara, A. Camposeo, G. Potente, E. Mele, R. Cingolani and D. Pisignano, *Adv. Funct. Mater.*, 2011, **21**, 1140.
13 A. Asthana, K.-O. Kim, J. Perumal, D.-M. Kim and D.-P. Kim, *Lab Chip*, 2009, **9**, 1138.
14 R. Sordan, A. Miranda, F. Traversi, D. Colombo, D. Chrastina, G. Isella, M. Masserini, L. Miglio, K. Kern and K. Balasubramanian, *Lab Chip*, 2009, **9**, 1556.
15 L. C. Campbell, M. J. Wilkinson, A. Manz, P. Camilleri and C. J. Humphreys, *Lab Chip*, 2004, **4**, 225.
16 D. M. Longo, W. E. Benson, T. Chraska and R. Hull, *Appl. Phys. Lett.*, 2001, **78**, 981.
17 H.-W. Li, D.-J. Kang, M. G. Blamire and W. T. S. Huck, *Nanotechnology*, 2003, **14**, 220.
18 T. Maleki, S. Mohammadi and B. Ziaie, *Nanotechnology*, 2009, **20**, 105302.
19 A. Imre, L. E. Ocola, L. Rich and J. Klingfus, *J. Vac. Sci. Technol., B: Microelectron. Nanometer Struct.–Process., Meas., Phenom.*, 2010, **28**, 304.
20 H. D. Wanzenboeck, M. Fischer, S. Mueller and E. Bertagnolli, *IEEE Sens. 2004*, 2004, **1–3**, 227.
21 J. J. Lai, K. E. Nelson, M. A. Nash, A. S. Hoffman, P. Yager and P. S. Stayton, *Lab Chip*, 2009, **9**, 1997.
22 N. Pamme, R. Koyama and A. Manz, *Lab Chip*, 2003, **3**, 187.
23 L. J. Steinbock, O. Otto, D. R. Skarstam, S. Jahn, C. Chimerel, J. L. Gornall and U. F. Keyser, *J. Phys.: Condens. Matter*, 2010, **22**, 454113.
24 H. Zhang, C. H. Chon, X. Pan and D. Li, *Microfluid. Nanofluid.*, 2009, **7**, 739.
25 M. A. McClain, C. T. Culbertson, S. C. Jacobson and J. M. Ramsey, *Anal. Chem.*, 2001, **73**, 5334.
26 A. M. Berezhkovskii1, G. Hummer and S. M. Bezrukov, *Phys. Rev. Lett.*, 2006, **97**, 020601.
27 L. J. Steinbock, O. Otto, C. Chimerel, J. Gornall and U. F. Keyser, *Nano Lett.*, 2010, **10**, 2493.
28 L. I. Segerink, A. J. Sprenkels, P. M. ter Braak, I. Vermes and A. van den Berg, *Lab Chip*, 2010, **10**, 1018.
29 D. Andreyev and E. A. Arriaga, *Anal. Chem.*, 2007, **79**, 5474.
30 O. Otto, F. Czerwinski, J. L. Gornall, G. Stober, L. B. Oddershede, R. Seidel and U. F. Keyser, *Opt. Express*, 2010, **18**, 22722.
31 J. C. Gadd, C. L. Kuyper, B. S. Fujimoto, R. W. Allen and D. T. Chiu, *Anal. Chem.*, 2008, **80**, 3450.
32 C. L. Kuyper, K. L. Budzinski, R. M. Lorenz and D. T. Chiu, *J. Am. Chem. Soc.*, 2006, **128**, 730.
33 H. B. Steen, *Cytometry, Part B*, 2004, **57A**, 94.
34 Y. H. Rezenom, A. D. Wellman, L. Tilstra, C. D. Medley and S. D. Gilman, *Analyst*, 2007, **132**, 1215.
35 K. J. O'Callaghan, A. J. Paine and A. Rudin, *J. Appl. Polym. Sci.*, 1995, **58**, 2047.
36 E. Kumacheva, O. Kalinina and L. Lilge, *Adv. Mater.*, 1999, **11**, 231.
37 K. C. Tang, E. Liao, W. L. Ong, J. D. S. Wong, A. Agarwal, R. Nagarajan and L. Yobas, *J. Phys. Conf. Ser.*, 2006, **34**, 155.
38 H. Bruus, *Theoretical microfluidics*, Oxford University Press, Oxford, 2008.
39 F. Zarrin and N. J. Dovichi, *Anal. Chem.*, 1987, **59**, 846.

